

Benchmarking Supercomputers with the Jülich Universal Quantum Computer Simulator

Dennis Willsch^{1,2}, Hannes Lagemann^{1,2}, Madita Willsch^{1,2}, Fengping Jin¹,
Hans De Raedt³, and Kristel Michielsen^{1,2}

¹ Institute for Advanced Simulation
Jülich Supercomputing Centre
Forschungszentrum Jülich
52425 Jülich, Germany

E-mail: {d.willsch, h.lagemann, m.willsch, f.jin, k.michielsen}@fz-juelich.de

² RWTH Aachen University
52056 Aachen, Germany

³ Zernike Institute for Advanced Materials
University of Groningen
Nijenborgh 4, NL-9747 AG Groningen, The Netherlands
E-mail: deraedthans@gmail.com

We use a massively parallel simulator of a universal quantum computer to benchmark some of the most powerful supercomputers in the world. We find nearly ideal scaling behavior on the Sunway TaihuLight, the K computer, the IBM BlueGene/Q JUQUEEN, and the Intel Xeon based clusters JURECA and JUWELS. On the Sunway TaihuLight and the K computer, universal quantum computers with up to 48 qubits can be simulated by means of an adaptive two-byte encoding to reduce the memory requirements by a factor of eight. Additionally, we discuss an alternative approach to alleviate the memory bottleneck by decomposing entangling gates such that low-depth circuits with a much larger number of qubits can be simulated.

1 Introduction

The simulation of large universal quantum computers on digital computers is a difficult task since every increase in the number of simulated qubits by one corresponds to a multiplication of the required amount of memory by a factor of two. A simulation of a universal quantum computer with 45 qubits requires slightly more than 0.5 PB (0.5×10^{15} bytes) of memory. There exist only a few digital computers with this amount of memory and a powerful network connecting a large number of compute nodes¹. Benchmarking such systems requires simulation software that can efficiently utilize the architecture of present day supercomputers. We present benchmarks of some of the most powerful supercomputers using the Jülich universal quantum computer simulator (JUQCS). A survey of JUQCS including its instruction set as well as benchmarks for Shor’s algorithm² and the adder circuit³ can be found in Ref. 4. JUQCS has also been used in the recent quantum supremacy experiments⁵.

In this article, we use the term “universal quantum computer” for the theoretical pen-and-paper version of a gate-based quantum computer⁶, in which the operation of the device is defined in terms of simple, sparse unitary matrices, representing the quantum gates, acting on state vectors, without any reference to the real time evolution of physical systems.

	JUQUEEN	K computer	Sunway TaihuLight	JURECA	JUWELS
CPU	IBM PowerPC A2	eight-core SPARC64 VIIIfx	SW26010 manycore 64-bit RISC	Intel Xeon E5-2680 v3	Dual Intel Xeon Platinum 8168
clock frequency	1.6 GHz	2.0 Ghz	1.45 GHz	2.5 GHz	2.7 GHz
memory/node	16 GB	16 GB	32 GB	128 GB	96 GB
# threads/core used	1 – 2	8	1	1 – 2	1 – 2
# cores used	1 – 262144	2 – 65536	1 – 131072	1 – 6144	1 – 98304
# nodes used	1 – 16384	2 – 65536	1 – 32768	1 – 256	1 – 2048
# MPI processes used	1 – 524288	2 – 65536	1 – 131072	1 – 1024	1 – 2048
# qubits	46 (43)	48 (45)	48 (45)	43 (40)	46 (43)

Table 1. Overview of the computer systems used for benchmarking. The IBM Blue Gene/Q JUQUEEN¹⁴ (decommissioned), JURECA¹⁵, and JUWELS¹⁶ are located at the Jülich Supercomputing Centre in Germany, the K computer at the RIKEN Center for Computational Science in Kobe, Japan, and the Sunway TaihuLight¹⁷ at the National Supercomputer Center in Wuxi, China. The row “# qubits” gives the maximum number of qubits that can be simulated with JUQCS–A (JUQCS–E). On JUWELS, the maximum number of qubits was limited to 43 (40) at the time of running the benchmarks.

In particular, we use the word “universal” to refer to a simulation of the full state vector, independent of the particular quantum circuit, representing an algorithm in terms of a sequence of gates operated on the qubits. In addition, we explore a complimentary simulation approach that allows for an efficient simulation of a much larger number of qubits for low-depth circuits if only a subset of all amplitudes is required (see also Refs. 7–12, 5).

Since the first massively parallel version of JUQCS was presented in 2007¹³, supercomputers have evolved significantly. Therefore, we have considered it timely to review and improve the computationally critical parts of the software and use it to benchmark some of the most powerful supercomputers that are operational today. The characteristics of the supercomputers that we have used for our benchmarks are summarized in Table 1.

JUQCS is portable software for digital computers and is based on Fortran 2003 code that was developed in 2007¹³. The revised version includes new operations to implement error-correction schemes and a parser for circuits specified in new quantum assembly flavors such as OpenQASM^{18,19}. JUQCS converts a quantum circuit into a form that is suitable for the simulation of the real-time dynamics of physical qubit models, such as NMR quantum computing²⁰ or quantum computer hardware based on superconducting circuits²¹.

The present version of JUQCS comes in two flavors. The first version, denoted by JUQCS–E, uses double precision (8-byte) floating point arithmetic and can be considered numerically exact (indicated by the E in the acronym). It has been used to simulate universal quantum computers with up to 45 qubits. The 45 qubit limit is only set by the amount of RAM memory available on the supercomputers listed in Table 1 (a universal simulation of N qubits using JUQCS–E requires slightly more than 2^{N+4} bytes).

A second version, denoted by JUQCS–A, trades memory for additional CPU time and has been used to simulate a universal quantum computer with up to 48 qubits. JUQCS–A uses adaptive coding to represent each amplitude of the quantum state with only two bytes⁴. This effectively reduces the memory requirements by a factor of eight relative to the one of JUQCS–E. The price to pay is a slightly longer execution time and a somewhat reduced numerical precision. However, we have found that the reduced precision (about 3 digits) is sufficiently accurate for all standard quantum circuits⁴.

We use the acronym JUQCS to refer to both versions of the software, while JUQCS–

E and JUQCS–A are used to specifically refer to the numerically exact version and the version using adaptive coding, respectively. Since portability was an important design objective, we have so far refrained from using machine-specific programming. A separate version of JUQCS–E utilizing the potential of GPUs is under development.

The memory bottleneck can be alleviated by decomposing entangling two-qubit gates (entangling gates)⁴. This trick can be used to great advantage if the number of entangling gates is not too large and if only a few of the coefficients of the final state vector need to be computed. The same idea has proven to be very useful in quantum Monte Carlo simulations²². Similar approaches have also been explored by other groups to simulate large random circuits with low depth^{7,8,10–12}.

2 Simulating Universal Quantum Computers with JUQCS

In quantum theory, the state of a single qubit is represented by two complex numbers a_0 and a_1 which are normalized such that $|a_0|^2 + |a_1|^2 = 1$. A gate operation on the qubit changes these numbers according to

$$\begin{pmatrix} a_0 \\ a_1 \end{pmatrix} \leftarrow U \begin{pmatrix} a_0 \\ a_1 \end{pmatrix}, \quad (1)$$

where U is a unitary 2×2 matrix. The state of N qubits is represented by a vector of 2^N complex numbers. Gate operations involving N qubits correspond to matrix-vector multiplications involving $2^N \times 2^N$ unitary matrices (see Ref. 6 for more information).

Typically, an N -qubit gate is expressed in terms of single-qubit gates (i.e., 2×2 matrices such as U in Eq. (1)) or two-qubit gates, which only act on a subset of the qubits. Therefore, the matrices required to simulate N -qubit circuits are extremely sparse. In other words, a quantum gate circuit for a universal quantum computer is, in essence, a representation of several extremely sparse matrix-vector operations. This means that only a few arithmetic operations are required to update each of the 2^N coefficients of the state vector. Therefore, in principle, simulating universal quantum computers is rather simple as long as there is no need to use distributed memory and the access to the shared memory is sufficiently fast^{23–26}. In practice, the speed to perform such operations is mainly limited by the bandwidth to (cache) memory.

For a large number of qubits, however, the only viable way to keep track of the 2^N complex coefficients is to use distributed memory, which comes at the expense of overhead due to communication between nodes, each of which can have several cores that share the memory (as is the case for all machines listed in Table 1). This makes up the “complicated” part of JUQCS that implements the MPI communication scheme. As described in Ref. 13, JUQCS reduces the communication overhead by minimizing the transfer of data between nodes. As JUQCS can be configured to use a combination of OpenMP and MPI to especially tax the processors, the memory, the communication network, or any combination of these, it provides a practical framework to benchmark high-performance computers.

3 Validation and Benchmarking

To validate the operation of JUQCS, we have executed standard quantum algorithms as well as random circuits using all gates from the JUQCS instruction set for $N \leq 30$ qubits

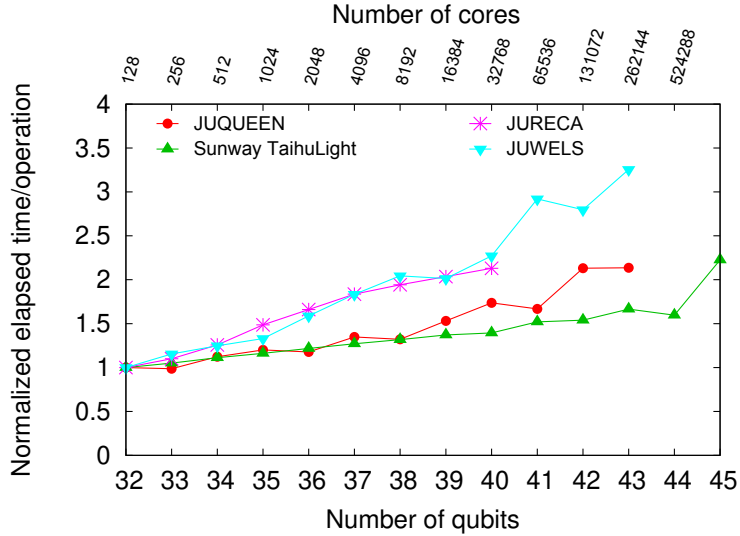


Figure 1. Weak scaling plot of JUQCS–E executing a Hadamard operation on qubit 0 and the sequence (CNOT 0 1), (CNOT 1 2), ..., (CNOT N-2, N-1), followed by a measurement of the expectation values of all qubits. Shown is the elapsed time per gate operation as a function of the number of qubits (normalized by the values corresponding to $N = 32$, i.e., 1.0 s (JUQUEEN), 5.1 s (Sunway TaihuLight), 1.4 s (JURECA), and 0.9 s (JUWELS)).

on both Windows and Linux systems. Validating the operation of JUQCS–E (JUQCS–A) when N reaches the limits $N = 45$ ($N = 48$), set by the amount of RAM available (see Table 1), is less trivial because of the requirement to use both MPI and OpenMP on distributed memory systems. For this reason, we made use of quantum circuits for which the exact outcome is known. In this article, we only present results for two particular representatives of such circuits since they are well suited to the purpose of benchmarking supercomputers. A more extensive discussion of the algorithms that were used to validate the operation and study the weak scaling behavior of JUQCS is given elsewhere⁴.

The first circuit that we consider is the circuit that creates a uniform superposition over all 2^N basis states by performing a Hadamard gate on each of the N qubits. Since the number of states is too large to be verified by sampling, a practical method to check the result is to compute the single-qubit expectation values $\langle Q_\alpha(i) \rangle = (1 - \sigma_i^\alpha)/2$ where σ_i^α for $\alpha = x, y, z$ denotes the Pauli matrix on qubit i , the exact values being 0 for $\alpha = x$ and 1/2 for $\alpha = y, z$. In this case, also JUQCS–A can compute the exact result since the encoding scheme is capable of representing the required amplitudes exactly⁴.

The second circuit is designed to create the maximally entangled state $(|0 \dots 0\rangle + |1 \dots 1\rangle)/\sqrt{2}$ by performing a Hadamard operation on the first qubit and a sequence of successive CNOT gates on qubits i and $i + 1$ for $i = 0, 1, \dots, N - 2$. Weak scaling results of executing this circuit on the supercomputer systems listed in Table 1 are shown in Fig. 1 (JUQCS–E) and Fig. 2 (JUQCS–A).

We see that JUQCS beats the exponential increase in run time with the number of qubits by doubling the computational resources with each added qubit. The weak scaling behavior

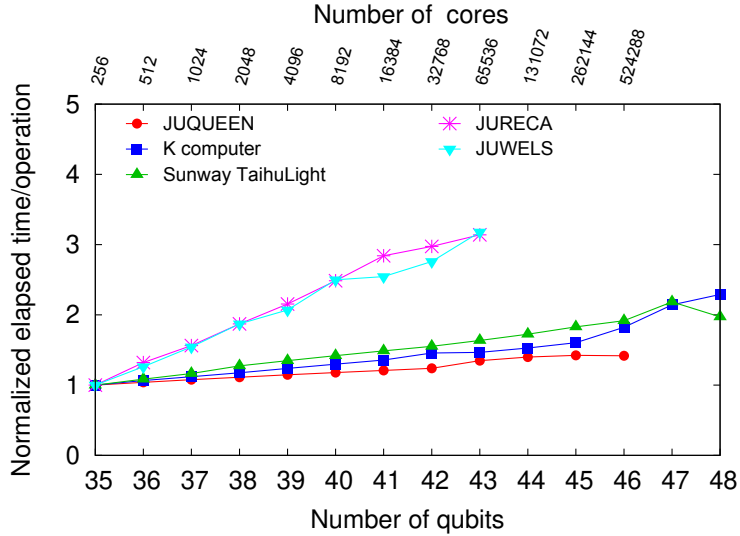


Figure 2. Weak scaling plot of JUQCS–A executing a Hadamard operation on qubit 0 and the sequence (CNOT 0 1), (CNOT 1 2), ..., (CNOT N-2, N-1), followed by a measurement of the expectation values of all qubits. Shown is the elapsed time per gate operation as a function of the number of qubits (normalized by the values corresponding to $N = 35$, i.e., 2.7 s (JUQUEEN), 3.8 s (K), 19.9 s (Sunway TaihuLight), 2.4 s (JURECA), and 2.2 s (JUWELS)).

on the Sunway TaihuLight, the K computer, and JUQUEEN is close-to-ideal. However, the weak scaling behavior on JURECA and JUWELS is not as good as the ones on the other supercomputers. Since the arithmetic work required for the Hadamard gate and the CNOT gate is rather low, the performance is mainly limited by the memory bandwidth. This suggests that there may be some limitations in the bandwidth to the memory and network on JURECA and JUWELS, compared to the other systems used in our benchmark. The best absolute run time is observed on JUWELS, closely followed by the other systems except the Sunway TaihuLight, which takes approximately four times longer.

Comparing Figs. 1 and 2, we also find that the computation time for JUQCS–E and JUQCS–A only differs by a factor of 1–4. The additional time for JUQCS–A is due to the encoding-decoding operation, which in turn affects the ratio between computation and communication. However, the additional time depends on the type of quantum gate. It can range, e.g., from almost zero for the CNOT gate to a factor of 2–3 for the Hadamard gate. As a result, comparing the computation times of JUQCS–A and JUQCS–E only makes sense for the same quantum circuit and even then, because of the difference in the number of qubits and the memory usage, interpreting differences in the elapsed times is not straightforward.

4 Memory Reduction by Decomposing Entangling Gates

There are many ways to alleviate the memory bottleneck. They are typically based on tensor-network contractions and (Schmidt) decompositions of two-qubit gates (cf. Refs. 7,

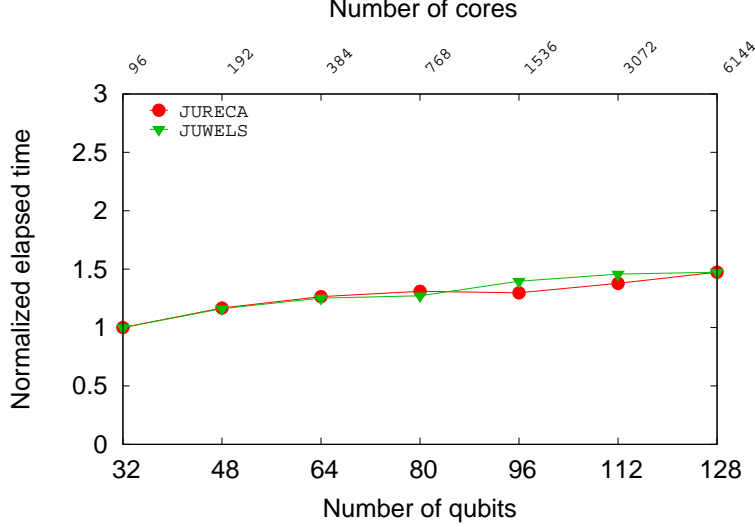


Figure 3. Scaling plot of a program implementing the memory reduction scheme according to Eq. (3), executing the same circuit as in Figs. 1 and 2. Shown is the elapsed time per gate operation as a function of the number of qubits (normalized by the values corresponding to $N = 32$, i.e., 2.12 s (JURECA) and 2.10 s (JUWELS)).

8, 10–12). In this section, we adopt an approach based on the decomposition of entangling gates using a discrete version of the Hubbard-Stratonovich transformation that has been used to great advantage in quantum Monte Carlo simulations²².

We start by expressing all entangling gates of an arbitrary circuit C in terms of single-qubit gates and the two-qubit CZ gate, which is always possible⁶. The action of the CZ gate on qubit i and qubit j (denoted by $\text{CZ}_{i,j}$) is defined as a sign flip of all coefficients with both qubits i and j in state $|1\rangle$. This action corresponds to the diagonal matrix $e^{i\pi(1+\sigma_i^z\sigma_j^z-\sigma_i^z-\sigma_j^z)/4}$, which can be decomposed into a sum of single-qubit operations according to

$$\text{CZ}_{i,j} = \frac{1}{2} \sum_{s \in \{-1,1\}} e^{i(\sigma_i^z + \sigma_j^z)(xs - \pi/4)}, \quad (2)$$

where x is a solution of $\cos(2x) = i$.

We partition all qubits $j = 0, \dots, N - 1$ into P mutually exclusive subsets labeled by $p = 0, \dots, P - 1$. The dimension of the corresponding subspace is denoted by $2 \leq D_p \leq 2^N$. If we decompose all CZ gates between different partitions p according to Eq. (2), we can express the circuit C as a sum of smaller subcircuits, $C = \sum_{s \in \{-1,1\}^S} \bigotimes_{p=0}^{P-1} W_p(s)$, where $S \in \mathbb{N}$ denotes the total number of decomposed CZ gates, and $W_p(s)$ is a subcircuit that only acts on qubits in the partition p . Each subcircuit (a.k.a. simulation path) can be simulated independently with a quantum computer simulator such as JUQCS-E or JUQCS-A. Note that in the extreme case where all CZ gates are decomposed, we have $P = N$, $D_p = 2$, and $W_p(s)$ is a product of single-qubit gates on qubit $j = p$ only.

The quantum computer is initialized in the state $|0\rangle$ of the computational basis. Consequently, the expression for the coefficient corresponding to the bit string \mathbf{z} of the final state

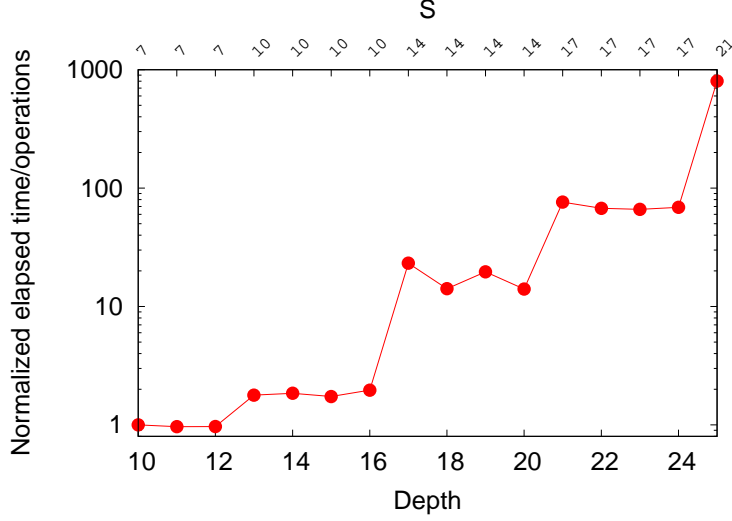


Figure 4. Scaling plot of a program implementing the memory reduction scheme according to Eq. (3), executing a set of random circuits for 42 qubits as a function of the circuit depth on JURECA. Shown is the elapsed time per gate operation, normalized by 0.0027 s corresponding to circuit depth 10. The axis on top of the figure shows the number S of decomposed entangling gates. The total number of gates ranges from 317 (depth 10) to 708 (depth 25). The circuits have been partitioned into two subcircuits of 21 qubits. The number of extracted coefficients is $M = 2^{20}$.

vector is given by

$$\langle \mathbf{z} | C | \mathbf{0} \rangle = \sum_{\mathbf{s} \in \{-1, 1\}^S} \prod_{p=0}^{P-1} \langle \mathbf{z}_p | W_p(\mathbf{s}) | \mathbf{0}_p \rangle, \quad (3)$$

where \mathbf{z}_p denotes the part of \mathbf{z} belonging to the qubits contained in the partition p .

From Eq. (3) it follows that memory reduction can be achieved by separating the circuit into a sum of P subcircuits acting only on a D_p -dimensional subspace of the large 2^N -dimensional space. The computation of $\langle \mathbf{z}_p | W_p(\mathbf{s}) | \mathbf{0}_p \rangle$ requires memory bound by the dimension D_p of this subspace. Obviously, reducing the memory requirements increases the number S of decomposed entangling gates and, consequently, also the computation time. This increase can be controlled by the choice of the P partitions.

A salient feature of the algorithm is that each term of the sum in Eq. (3) is independent. We have parallelized this sum using MPI to reduce the elapsed time by distributing the work on more cores. Furthermore, the evaluation of all $W_p(\mathbf{s})$'s is parallelized with OpenMP. If more than one coefficient of the final state vector is requested, a list of M coefficients $\{\langle \mathbf{z} | C | \mathbf{0} \rangle\}$ can be computed in a single run. The reason for this is that computations for different coefficients only differ by the index of the coefficient extracted from the vector $W_p(\mathbf{s}) | \mathbf{0}_p \rangle$. Thus $W_p(\mathbf{s}) | \mathbf{0}_p \rangle$ needs to be computed once for each partition p and M determines the number of coefficients extracted from this result.

In summary, this algorithm has a worst-case time complexity of $\mathcal{O}(2^S P \max\{D_p, M\} / RT)$ and a worst-case space complexity of $\mathcal{O}(R \max\{D_p, M\})$,

where R denotes the number of MPI processes, T denotes the number of OpenMP threads, and M is the desired number of coefficients from the final state vector.

In Fig. 3, we present scaling results for the circuit used for Figs. 1 and 2, up to a maximum of $N = 128$ qubits and $M = 2^{27}$ extracted coefficients. The two coefficients corresponding to the states $|0 \dots 0\rangle$ and $|1 \dots 1\rangle$ are $1/\sqrt{2}$, as expected. Qualitatively, the scaling behavior of the algorithm on JURECA and JUWELS is nearly identical. Only the data points for the qubit numbers 80, 96, and 112 show small differences. Since all normalized run times are between 1 and 1.5, both JURECA and JUWELS show almost ideal scaling, suggesting that the previously observed limitations do not play a role for this kind of problem.

As the results presented in Fig. 3 are based on a circuit for which only a small number of entangling gates need to be decomposed, we also present results for a set of random quantum circuits, generated according to the procedure given by Boixo et al.²⁷. The circuits are characterized by their depth, which is the maximum number of layers (also called clock cycles or circuit moments) when all consecutive gates on different qubits are grouped into a single layer. These circuits pose a more difficult problem for the decomposition algorithm because the control and target qubits of the CZ gates are distributed in such a way that one cannot partition the circuit into smaller subcircuits without at least doubling the size S of decomposed entangling gates. Furthermore, the density of single-qubit gates is high. Consequently, at some point, increasing the number of MPI processes will not prevent the elapsed time from growing exponentially. In this respect, all algorithms based on a memory reduction using similar ideas^{7,8,10-12} differ from the universal simulator JUQCS in that the scaling observed for JUQCS is almost independent of the particular circuit simulated.

Figure 4 shows the normalized elapsed run times per operation for random circuit simulations as a function of the circuit depth. The number of simulated qubits is 42. We find that for circuits with a low depth, the run time is quasi constant because enough computational resources are available to distribute the work. For circuits with depth 13 and larger, we always use the same amount of computational resources, namely 512 MPI processes and 48 OpenMP threads per process. Consequently, we see a step-like increase in the run time at depth 17, 21, and 25. These results show that, within reasonable fluctuations, the run time scales according to the time complexity discussed above when the parameters D_p , R , and T are held constant and only S changes.

5 Conclusion

The massively parallel quantum computer simulator JUQCS has been used to benchmark the Sunway TaihuLight¹⁷, the K computer, the IBM BlueGene/Q JUQUEEN¹⁴, and the Intel Xeon based clusters JURECA¹⁵ and JUWELS¹⁶ by simulating quantum circuits with up to $N = 48$ qubits. We observed close-to-linear scaling of the elapsed time as a function of the number of qubits on all tested supercomputers. The scaling performance on JUQUEEN, the Sunway TaihuLight, and the K computer tends to be better than on JURECA and JUWELS, suggesting some limitations in the bandwidth of the latter. The absolute execution times were best on JUWELS, closely followed by JUQUEEN, JURECA, and the K computer. The simulation on the Sunway TaihuLight was approximately four times slower.

Two methods to circumvent the memory problem associated with the simulation of

quantum systems on a digital computer have been explored. The first uses an adaptive coding scheme to represent the quantum state in terms of 2-byte instead of 16-byte numbers. We observed that the reduction in memory has no significant impact on the accuracy of the outcomes (see also Ref. 4).

The second method uses a technique known from Quantum Monte Carlo simulations to express two-qubit gates in terms of sums of single-qubit gates. Using this technique, we observed nearly ideal scaling on JURECA and JUWELS for a maximally entangling circuit with up to $N = 128$ qubits. Additionally, we used the method to simulate random 42-qubit circuits up to depth 25.

As the new generation of high-performance computers relies on accelerators or GPUs to deliver even more FLOPS, we have started to develop a CUDA-based version of JUQCS to explore and benchmark the potential of using GPUs for simulating universal quantum computers.

Since JUQCS can easily be configured to put a heavy burden on the processors, the memory, the communication network, or any combination of them, it may be a useful addition to the suite of benchmarks for high-performance computers.

Acknowledgments

We thank Koen De Raedt for his help in improving the JUQCS code. The authors acknowledge the computing time granted by the JARA-HPC Vergabegremium and provided on the JARA-HPC Partition part of the supercomputers JURECA¹⁵ and JUQUEEN¹⁴ at the Forschungszentrum Jülich. The authors gratefully acknowledge the Gauss Centre for Supercomputing e.V. (www.gauss-centre.eu) for funding this project by providing computing time on the GCS Supercomputer JUWELS¹⁶ at Jülich Supercomputing Centre (JSC). D.W. is supported by the Initiative and Networking Fund of the Helmholtz Association through the Strategic Future Field of Research project “Scalable solid state quantum computing (ZT-0013)”. Part of the simulations reported in this paper were carried out on the K computer at RIKEN Center for Computational Science in Kobe, Japan, and the Sunway TaihuLight¹⁷ at the National Supercomputer Center in Wuxi, China.

References

1. “Top500”, <https://www.top500.org/>.
2. P. W. Shor, *Polynomial-Time Algorithms for Prime Factorization and Discrete Logarithms on a Quantum Computer*, SIAM Review, **41**, 303, 1999.
3. T. G. Draper, *Addition on a Quantum Computer*, arXiv:quant-ph/0008033, 2000.
4. H. De Raedt, F. Jin, D. Willsch, M. Willsch, N. Yoshioka, N. Ito, S. Yuan, and K. Michielsen, *Massively parallel quantum computer simulator, eleven years later*, Comput. Phys. Commun., **237**, 47 – 61, 2019.
5. Frank Arute, Kunal Arya, Ryan Babbush, Dave Bacon, Joseph C. Bardin, Rami Barends, Rupak Biswas, Sergio Boixo, Fernando G. S. L. Brandao, David A. Buell, Brian Burkett, Yu Chen, Zijun Chen, Ben Chiaro, Roberto Collins, William Courtney, Andrew Dunsworth, Edward Farhi, Brooks Foxen, Austin Fowler, Craig Gidney, Marissa Giustina, Rob Graff, Keith Guerin, Steve Habegger, Matthew P. Harrigan, Michael J. Hartmann, Alan Ho, Markus Hoffmann, Trent Huang, Travis S.

- Humble, Sergei V. Isakov, Evan Jeffrey, Zhang Jiang, Dvir Kafri, Kostyantyn Kechedzhi, Julian Kelly, Paul V. Klimov, Sergey Knysh, Alexander Korotkov, Fedor Kostritsa, David Landhuis, Mike Lindmark, Erik Lucero, Dmitry Lyakh, Salvatore Mandrà, Jarrod R. McClean, Matthew McEwen, Anthony Megrant, Xiao Mi, Kristel Michielsen, Masoud Mohseni, Josh Mutus, Ofer Naaman, Matthew Neeley, Charles Neill, Murphy Yuezhen Niu, Eric Ostby, Andre Petukhov, John C. Platt, Chris Quintana, Eleanor G. Rieffel, Pedram Roushan, Nicholas C. Rubin, Daniel Sank, Kevin J. Satzinger, Vadim Smelyanskiy, Kevin J. Sung, Matthew D. Trevithick, Amit Vainsencher, Benjamin Villalonga, Theodore White, Z. Jamie Yao, Ping Yeh, Adam Zalcman, Hartmut Neven, and John M. Martinis, *Quantum supremacy using a programmable superconducting processor*, *Nature*, **574**, 505–510, 2019.
6. M. Nielsen and I. Chuang, *Quantum Computation and Quantum Information*, Cambridge University Press, Cambridge, 10th anniversary edition, 2010.
 7. E. Pednault, J. A. Gunnels, G. Nannicini, L. Horesh, T. Magerlein, E. Solomonik, and R. Wisnieff, *Breaking the 49-Qubit Barrier in the Simulation of Quantum Circuits*, arXiv:1710.05867, 2017.
 8. S. Boixo, S. V. Isakov, V. N. Smelyanskiy, and H. Neven, *Simulation of low-depth quantum circuits as complex undirected graphical models*, arXiv:1712.05384, 2017.
 9. Jianxin Chen, Fang Zhang, Cupjin Huang, Michael Newman, and Yaoyun Shi, *Classical Simulation of Intermediate-Size Quantum Circuits*, arXiv:1805.01450, 2018.
 10. Z. Chen, Q. Zhou, C. Xue, X. Yang, G. Guo, and G. Guo, *64-qubit quantum circuit simulation*, *Sci. Bull.*, pp. 964 – 971, 2018.
 11. I. L. Markov, A. Fatima, S. V. Isakov, and S. Boixo, *Quantum Supremacy Is Both Closer and Farther than It Appears*, arXiv:1807.10749, 2018.
 12. B. Villalonga, D. Lyakh, S. Boixo, H. Neven, T. S. Humble, R. Biswas, E. G. Rieffel, A. Ho, and S. Mandrà, *Establishing the Quantum Supremacy Frontier with a 281 Pflop/s Simulation*, arXiv:1905.00444, 2019.
 13. K. De Raedt, K. Michielsen, H. De Raedt, B. Trieu, G. Arnold, M. Richter, Th. Lipfert, H. Watanabe, and N. Ito, *Massively parallel quantum computer simulator*, *Comput. Phys. Commun.*, **176**, 121 – 136, 2007.
 14. Jülich Supercomputing Centre, *JUQUEEN: IBM Blue Gene/Q Supercomputer System at the Jülich Supercomputing Centre*, *J. of Large-Scale Res. Facil.*, **1**, A1, 2015.
 15. Jülich Supercomputing Centre, *JURECA: Modular supercomputer at Jülich Supercomputing Centre*, *J. of Large-Scale Res. Facil.*, **4**, A132, 2018.
 16. Jülich Supercomputing Centre, *JUWELS: Modular Tier-0/1 Supercomputer at the Jülich Supercomputing Centre*, *J. of Large-Scale Res. Facil.*, **5**, A135, 2019.
 17. W. Zhang, J. Lin, W. Xu, H. Fu, and G. Yang, *SCStore: Managing Scientific Computing Packages for Hybrid System with Containers*, *Tsinghua Science and Technology*, **22**, 675 – 681, 2017.
 18. IBM Q, “Quantum experience”, <https://www.research.ibm.com/ibm-q/>, 2016.
 19. A. W. Cross, L. S. Bishop, J. A. Smolin, and J. M. Gambetta, *Open Quantum Assembly Language*, arXiv:1707.03429, 2017.
 20. H. De Raedt, K. Michielsen, A. Hams, S. Miyashita, and K. Saito, *Quantum Spin Dynamics as a Model for Quantum Computer Operation*, *Eur. Phys. J.*, **B27**, 15 – 28, 2002.

21. D. Willsch, M. Nocon, F. Jin, H. De Raedt, and K. Michielsen, *Gate-error analysis in simulations of quantum computers with transmon qubits*, Phys. Rev. A, **96**, 062302, 2017.
22. J. E. Hirsch, *Discrete Hubbard-Stratonovich transformation for fermion lattice models*, Phys. Rev. B, **28**, 4059–4061, 1983.
23. H. De Raedt and K. Michielsen, “Computational Methods for Simulating Quantum Computers”, in: Handbook of Theoretical and Computational Nanotechnology, M. Rieth and W. Schommers, (Eds.), pp. 2 – 48. American Scientific Publishers, Los Angeles, 2006.
24. A. Aspuru-Guzik M. Smelyanskiy, N. P. D. Sawaya, *qHiPSTER: The Quantum High Performance Software Testing Environment*, arXiv:1601.07195, 2016.
25. N. Khammassi, I. Ashraf, X. Fu, C. G. Almudever, and K. Bertels, *QX: A high-performance quantum computer simulation platform*, in: Design, Automation Test in Europe Conference Exhibition, pp. 464–469, 2017.
26. Th. Häner and D. S. Steiger, *0.5 Petabyte Simulation of a 45-qubit Quantum Circuit*, in: Proceedings of the International Conference for High Performance Computing, Networking, Storage and Analysis, SC '17, pp. 33:1–33:10, ACM. 2017.
27. S. Boixo, S. V. Isakov, V. N. Smelyanskiy, R. Babbush, N. Ding, Z. Jiang, M. J. Bremner, J. M. Martinis, and H. Neven, *Characterizing quantum supremacy in near-term devices*, Nat. Phys., **14**, 595–600, 2018.